Occupancy correlations in the asymmetric simple inclusion process

Ofek Lauber Bonomo and Shlomi Reuveni*

School of Chemistry, The Center for Physics and Chemistry of Living Systems, The Raymond and Beverly Sackler Center for Computational Molecular and Materials Science, and The Mark Ratner Institute for Single Molecule Chemistry, Tel Aviv University, Tel Aviv 6997801, Israel

The asymmetric simple inclusion process (ASIP)—a lattice-gas model for unidirectional transport with irreversible aggregation—has been proposed as an inclusion counterpart of the asymmetric simple exclusion process and as a batch service counterpart of the tandem Jackson network. To date, the analytical tractability of the model has been limited: while the average particle density in the model is easy to compute, very little is known about the joint occupancy distribution. To partially bridge this gap, we study occupancy correlations in the ASIP. We take an analytical approach to this problem and derive an exact formula for the covariance matrix of the steady-state occupancy vector. We verify the validity of this formula numerically in small ASIP systems, where Monte Carlo simulations can provide reliable estimates for correlations in reasonable time, and further use it to draw a comprehensive picture of spatial occupancy correlations in ASIP systems of arbitrary size.

I. INTRODUCTION

Many complex and fundamental processes in nature incorporate a high level of intrinsic randomness. Stochastic events stand at the very bedrock of their microlevel description, and the cumulative effect of these events is manifested in their dynamics and functionality. Complex processes may sometimes be viewed as an interconnected network whose basic building blocks are processes of diminished complexity. Interestingly, even when the isolated behavior of each building block is understood in great detail, the behavior of the aggregate can often be extremely hard to predict. A subclass of systems in which considerable progress has, nevertheless, been made is collectively referred to as tandem stochastic systems (TSSs)—linear stochastic networks formed by the sequential concatenation of relatively simple building blocks. The prevalence of TSS throughout the sciences renders this particular class of stochastic networks a special case of interest among a host of scientific communities.

Tandem stochastic systems are systems in which a stochastic input flow (of jobs, molecules, particles, etc.) progresses through a serial array of sites. The progress from one site to the next is governed by a set of rules characterizing the system's law of motion. TSS naturally emerge in many scientific fields, including biology, chemistry, physics, and operations research, and often exhibit complex stochastic dynamics. The existing body of knowledge on TSS is comprised of a small number of mathematical models that were introduced throughout the years. Each of these models was tailored to describe a different tandem stochastic system. Facing the significant complexity that is inherent to the analysis of TSS in general, this somewhat *ad hoc* approach is still considered inevitable.

This paper presents new results for occupancy correlations in the asymmetric simple inclusion process (ASIP)—a TSS which serves as a lattice-gas model for unidirectional transport with irreversible aggregation [1,2]. Before discussing the ASIP, we provide a brief overview of two other TSSs: (i) the tandem Jackson network (TJN) and (ii) the asymmetric simple exclusion process (ASEP). These well-known TSSs are strongly related to the ASIP and reviewing them will help put the findings presented here in context.

A. The tandem Jackson network

The TJN is one of the first TSSs ever to be studied. It was introduced and analyzed by R. R. P. Jackson when he was working for the operational research branch of the London airport [3,4]. Jackson was inspired by a visit to a factory in which aircraft engines were overhauled. As he explains in the introduction to his paper:

> Work was carried out on the engines in successive stages, e.g. stripping, detailed examination, repairs, assembly and testing, and thus engines could experience inter-phase queueing. It was thought that a mathematical investigation into such a system would be helpful in planning future work and increasing the present efficiency. [An apology was then quick to come.] Unfortunately, to date, the only system of this type which appears to be mathematically tractable is one which is completely random in character, and this is now investigated.

In its simplest version, the TJN is a sequential array of n service stations, where external jobs arrive at the leftmost station randomly in time and progress sequentially from station to station. At each station, (i) arriving jobs queue up in line and await service; (ii) only one job is served at a time; (iii) service durations are random and come from an exponential distribution; and (iv) upon completion of service, a single job moves on to the next station or, in the case of the rightmost station, out of the system.

In the standard queueing theory setting, the TJN can be described as a sequential array of Markovian queues [5]. Jobs arrive to the first queue according to a Poisson process with

---

*shlomire@tauex.tau.ac.il

rate λ and are processed, one by one and according to order of arrival, with rate μ_k at station k. Denoting the number of jobs present in the kth station ($k = 1, \ldots, n$) by X_k, the TJN's dynamics can be schematically summarized as follows:

(i) the first station ($k = 1$),

$$X_1, X_2, \ldots \xrightarrow{\lambda} X_1 + 1, X_2, \ldots; \qquad (1)$$

(ii) interior stations (when $X_k > 0$, $1 < k \leqslant n - 1$),

$$\ldots, X_{k-1}, X_k, X_{k+1}, \ldots \xrightarrow{\mu_k} \ldots, X_{k-1}, X_k - 1, X_{k+1} + 1, \ldots; \qquad (2)$$

(iii) the last station (when $X_n > 0$),

$$\ldots, X_{n-1}, X_n \xrightarrow{\mu_n} \ldots, X_{n-1}, X_n - 1. \qquad (3)$$

When $n = 1$, the TJN is composed of a single service station which, using the notation introduced by Kendall [6], is equivalent to a simple $M/M/1$ queue. When $\lambda < \mu_1$, this queue is stable and its steady-state distribution is given by [5]

$$\Pr(X_1 = x_1) = (1 - \rho_1)\rho_1^{x_1}, \qquad (4)$$

where $\rho_1 = \lambda/\mu_1$ ($x_1 = 0, 1, 2, \ldots$). While this result was known to Jackson and his contemporaries, its extension to $n > 1$ stations was considered nontrivial. Indeed, when the output from one station is the input of the next, intricate correlations may (in principle) arise and render the joint probability distribution of the system extremely complex or even completely intractable.

In light of the above, it is quite remarkable that the steady-state distribution of a TJN with n service stations has the product form

$$\Pr(X_1 = x_1, \ldots, X_n = x_n) = \prod_{k=1}^{n}(1 - \rho_k)\rho_k^{x_k}, \qquad (5)$$

provided that $\rho_k = \lambda/\mu_k < 1$ ($x_k = 0, 1, 2, \ldots$). Equation (5) is known as Jackson's theorem; it asserts that stations in the TJN behave as if they were a collection of n separate $M/M/1$ queues that are statistically independent of each other. The great simplicity and elegance of this result are best appreciated when compared to the two other TSSs described hereinafter.

B. The asymmetric simple exclusion process

The ASEP is a paradigmatic unidirectional lattice-gas flow model in nonequilibrium statistical physics [7–10]. Having first appeared in the literature as a model of biopolymerization [11], it was later introduced to the probability theory and statistical-physics communities by Frank Spitzer [12] and has now become a default model for stochastic transport with excluded volume interactions. Over the years, the ASEP and its variants were used to study a wide range of physical phenomena: transport across membranes [13], transport of macromolecules through thin vessels [14], hopping conductivity in solid electrolytes [15], reptation of a polymer in a gel [16], traffic flow [17], protein synthesis by ribosomes [18,19], surface growth [20,21], sequence alignment [22], molecular motors [23], and the directed motion of tracer particles in the presence of dynamical backgrounds [24–27].

In the ASEP, particles flow randomly in time, into the leftmost site of a one-dimensional lattice, and propagate unidirectionally (to the right) along the lattice. Particles move from a site to its right-neighboring site randomly in time—the hopping restricted by the exclusion principle, which allows sites to be occupied by no more than one particle at a time. At the rightmost site, particles exit the system randomly in time. The exclusion principle causes jamming throughout the lattice and renders the ASEP's dynamics highly nontrivial.

The translation between the queueing-theory setting of the TJN and the statistical physics setting of the ASEP is straightforward: 'jobs' are 'particles' and 'service stations' are 'sites.' The random inflow into the leftmost site in the ASEP, the random instants of hopping from site to site, and the random outflow from the rightmost site are all governed by independent Poisson processes. Denoting an occupied site by a filled circle and an empty site by an open circle, the ASEP's dynamics can be schematically summarized as follows:

(i) first site ($k = 1$),

$$\circ, \cdots \xrightarrow{\lambda} \bullet, \cdots; \qquad (6)$$

(ii) interior sites ($1 < k \leqslant n - 1$),

$$\cdots, \bullet, \circ, \cdots \xrightarrow{\mu_k} \cdots, \circ, \bullet, \cdots; \qquad (7)$$

(iii) last site ($k = n$),

$$\cdots, \bullet \xrightarrow{\mu_n} \cdots, \circ. \qquad (8)$$

Recalling that the capacity of a queue is the maximum number of jobs allowed in it (including those in service), one can think of the ASEP as a TJN of Markovian queues with single job capacity. When this number is reached, further arrivals to the first site are turned away and blocking occurs in interior sites.

In contrast to the steady-state distribution of the TJN, that of the ASEP does not obey a product form, i.e., particle occupancies in distinct sites are statistically dependent. It is nevertheless interesting to note that exact expressions for the steady-state distribution can be put in the form of a matrix product. To this end, the statistical weight of each of the 2^n possible configurations of an ASEP lattice is constructed as a product of matrices, one for each site, chosen according to the state of the site (occupied or empty). The probability of observing the lattice in a particular configuration can then be obtained following proper normalization. A matrix-product solution for the steady-state distribution of the ASEP was first derived in Ref. [28]. Matrix-product forms are reviewed in Ref. [10].

C. The asymmetric simple inclusion process

The ASIP is a "bosonic" counterpart of the ASEP [1,2,29–31]. Namely, in the ASIP the number of particles that simultaneously occupy a given site is not limited. Moreover, and in contrast to the TJN discussed above, in the ASIP particles have an irreversible tendency to stick together. This principle is suitable for the description of physical systems whose behavior is opposite to that dictated by the exclusion principle of the ASEP. Indeed, while random events cause particles to propagate unidirectionally along a one-dimensional lattice in both the ASEP and the ASIP; In the ASEP particles are subject to *exclusion* interactions that keep them singled apart, whereas in the ASIP particles are subject to *inclusion* interactions that coalesce them into inseparable clusters. To avoid confusion, we note that there is also a different model with the name ASIP [32,33], which is not discussed here.

The formulation of the ASIP is as follows. Consider a one-dimensional lattice of n sites indexed $k = 1, \ldots, n$. Each site is followed by a gate—labeled by the site's index—which controls the site's outflow. Particles arrive at the first site ($k = 1$) following a Poisson process with rate λ, the openings of gate k are timed according to a Poisson process with rate μ_k ($k = 1, \ldots, n$), and the $n + 1$ Poisson processes are mutually independent. A key feature of the ASIP is its 'batch service' property: at an opening of gate k all particles present at site k transit simultaneously, and in one batch (one cluster), to site $k + 1$—thus joining particles that may already be present at site $k + 1$ ($k = 1, \ldots, n - 1$). At an opening of the last gate ($k = n$) all particles present at site n exit the lattice simultaneously. Denoting the number of particles present at site k ($k = 1, \ldots, n$) by X_k, the ASIP's dynamics can be schematically summarized as follows:

(i) first site ($k = 1$),

$$X_1, X_2, \ldots \xrightarrow{\lambda} X_1 + 1, X_2, \ldots; \tag{9}$$

(ii) interior sites ($1 < k \leqslant n - 1$),

$$\ldots, X_{k-1}, X_k, X_{k+1}, \ldots \xrightarrow{\mu_k} \ldots, X_{k-1}, 0, X_{k+1} + X_k, \ldots; \tag{10}$$

(iii) last site ($k = n$),

$$\ldots, X_{n-1}, X_n \xrightarrow{\mu_n} \ldots, X_{n-1}, 0. \tag{11}$$

From a queueing theory perspective, the ASIP is a sequential array of Markovian queues with unbounded capacity and unlimited batch service [34,35]: all particles present at a given service station are served collectively (and thus move together to the next service station or out of the system). The notion of 'batch service' is strongly related to growth-collapse processes. Consider a single service station with batch service. Jobs arrive at the station randomly in time, causing the queue to grow steadily; when service is rendered all jobs are served simultaneously, causing the queue to collapse to 0. Thus, stochastic growth-collapse temporal patterns emerge from the application of batch-service policies [34–38]. Interestingly, these patterns also appear in a variety of complex systems, including sand-pile models and systems in self-organized criticality [39], stick-slip models of interfacial friction [40], Burridge-Knopof-type models of earthquakes and continental drift [41], stochastic avalanche models [42], stochastic Ornstein-Uhlenbeck capacitors [43], and geometric Langevin equations [44]. The ASIP model is, in effect, a tandem array of growth-collapse processes.

From a statistical physics perspective, the ASIP is a model for unidirectional transport with irreversible aggregation and coagulation. Such reaction-diffusion models have been extensively studied since the pioneering work of Smoluchowski [45]. Still, unresolved issues and intriguing new facets cause them to raise interest even today [46,47]. Two of the simplest models of this kind are the coalescence-diffusion model,

$$\cdots \bullet \bullet \cdots \xrightarrow{1} \cdots \circ \bullet \cdots,$$

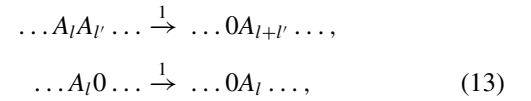$$\cdots \bullet \circ \cdots \xrightarrow{1} \cdots \circ \bullet \cdots, \tag{12}$$
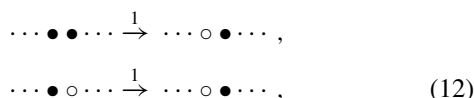
where a filled circle represents an occupied site and an open circle represents an empty site, and the aggregation-diffusion

TABLE I. Capacity classification of the TJN, ASEP, and ASIP models.

	$c_{\text{site}} = 1$	$c_{\text{site}} = \infty$
$c_{\text{gate}} = 1$	ASEP	TJN
$c_{\text{gate}} = \infty$	ASEP	ASIP

model,

$$\ldots A_l A_{l'} \ldots \xrightarrow{1} \ldots 0 A_{l+l'} \ldots,$$

$$\ldots A_l 0 \ldots \xrightarrow{1} \ldots 0 A_l \ldots, \tag{13}$$

where A_l represents a site occupied by $l > 0$ particles, and 0 represents an empty site [48].

The studies dedicated to the models described in Eqs. (12) and (13) were, by and large, carried out in a one-dimensional ring topology. Under these conditions, many statistical properties can be calculated exactly using the empty-interval method [48,49]. The ASIP, with homogeneous unit rates $\{\mu_1 = \cdots = \mu_n = 1\}$, can be viewed as a generalization of aggregation-diffusion models to an open system. Indeed, the bulk ASIP dynamics of Eq. (10) is identical to the dynamics of Eq. (13). Similarly, when one disregards the number of particles occupying each site (X_k) and focuses only on whether or not sites are occupied ($X_k > 0$ or $X_k = 0$), the ASIP dynamics turns into an open-boundary version of Eq. (12).

D. Connection between the TJN, ASEP, and ASIP

Interestingly, all three models—the TJN, ASEP, and ASIP—can be described by the sites-gates language that was used to describe the ASIP. To better understand the difference between the models consider the following two characteristic capacities: (i) the *site capacity* c_{site}—the maximal number of particles that can simultaneously occupy a given site; and (ii) the *gate capacity* c_{gate}—the maximal number of particles that are simultaneously transferred through a given gate when it opens. In each of the above-mentioned models particles propagate according to the following rule: at an opening of gate k, $\min(X_k, c_{\text{site}} - X_{k+1}, c_{\text{gate}})$ particles transit simultaneously from site k to site $k + 1$—thus joining particles that may already be present at site k ($k = 1, 2, \ldots, n - 1$). At an opening of the last gate ($k = n$), $\min(X_k, c_{\text{gate}})$ particles exit the lattice simultaneously. In the TJN the site capacity is $c_{\text{site}} = \infty$ and the gate capacity is $c_{\text{gate}} = 1$. In the ASIP the site capacity is $c_{\text{site}} = \infty$ and the gate capacity is $c_{\text{gate}} = \infty$. Finally, note that in the ASEP the site capacity is $c_{\text{site}} = 1$ and the gate capacity can be any positive integer $1 \leqslant c_{\text{gate}} \leqslant \infty$. Indeed, since $c_{\text{site}} = 1$ only one particle can occupy each site, which means that the overall dynamics is insensitive to the value taken by c_{gate}. The capacity classification is summarized in Table I—from which it is evident that the ASIP is, in effect, a 'missing puzzle piece' connecting the well-established and the well-studied ASEP and TJN models.

E. The asymmetric simple inclusion process: Fundamental results

Many fundamental results that were obtained for the ASIP made use of its Markovian dynamics, which we now describe.

Set $\mu_c = \mu_1 + \cdots + \mu_n$ to be the ASIP's cumulative hopping rate, let $X_k(t)$ denote the number of particles present at the kth site ($k = 1, \ldots, n$) at time t ($t \geqslant 0$), and set $\mathbf{X}(n, t) = (X_1(t), \ldots, X_n(t))^\top$. The vector $\mathbf{X}(n, t)$ represents the occupancy of an ASIP system with n sites at time t. Observe

the system at times t and $t' = t + \Delta$ (for small Δ) and use the shorthand notation $\mathbf{X} = \mathbf{X}(n, t)$ and $\mathbf{X}' = \mathbf{X}(n, t')$. The stochastic connection between the random vectors $\mathbf{X}$ and $\mathbf{X}'$ characterizing the Markovian 'law of motion' of the stochastic process $[\mathbf{X}(t)]_{t \geqslant 0}$ is given by

$$(X_1', \ldots, X_n') = \begin{cases} (X_1, X_2, X_3, \ldots, X_{n-1}, X_n) & \text{w.p.} \quad 1 - (\lambda + \mu_c)\Delta + o(\Delta), \\[8pt] (X_1 + 1, X_2, X_3, \ldots, X_{n-1}, X_n) & \text{w.p.} \quad \lambda\Delta + o(\Delta), \\[8pt] (0, X_1 + X_2, X_3, \ldots, X_{n-1}, X_n) & \text{w.p.} \quad \mu_1\Delta + o(\Delta), \\[8pt] (X_1, 0, X_2 + X_3, \ldots, X_{n-1}, X_n) & \text{w.p.} \quad \mu_2\Delta + o(\Delta), \\[8pt] \vdots & \quad \vdots \\[8pt] (X_1, X_2, X_3, \ldots, 0, X_{n-1} + X_n) & \text{w.p.} \quad \mu_{n-1}\Delta + o(\Delta), \\[8pt] (X_1, X_2, X_3, \ldots, X_{n-1}, 0) & \text{w.p.} \quad \mu_n\Delta + o(\Delta), \end{cases} \tag{14}$$

where w.p. stands for "with probability."

Equation (14) follows from considering the totality of events that may take place within the time interval $(t, t']$: (0) arrival of a particle at the first site occurring with probability $\lambda\Delta + o(\Delta)$, in which case $X_1 \mapsto X_1' = X_1 + 1$; (1) transition of all particles from the first site to the second site occurring with probability $\mu_1\Delta + o(\Delta)$, in which case $X_1 \mapsto X_1' = 0$ and $X_2 \mapsto X_2' = X_1 + X_2$; (2) transition of all particles from the second site to the third site occurring with probability $\mu_2\Delta + o(\Delta)$, in which case $X_2 \mapsto X_2' = 0$ and $X_3 \mapsto X_3' = X_2 + X_3$; $\ldots$; $(n-1)$ transition of all particles from the site before the last to the last site occurring with probability $\mu_{n-1}\Delta + o(\Delta)$, in which case $X_{n-1} \mapsto X_{n-1}' = 0$ and $X_n \mapsto X_n' = X_{n-1} + X_n$; and (n) transition of all particles from the last site to outside of the lattice occurring with probability $\mu_n\Delta + o(\Delta)$, in which case $X_n \mapsto X_n' = 0$. The first line on the right-hand-side of Eq. (14) represents the scenario in which no event takes place, which occurs with the complementary probability $1 - (\lambda + \mu_c)\Delta + o(\Delta)$.

At steady state, the stochastic process $[\mathbf{X}(t)]_{t \geqslant 0}$ is stationary, hence the means are time homogeneous: $\langle \mathbf{X}(n, t) \rangle \equiv \langle \mathbf{X}(n) \rangle$ ($t \geqslant 0$), where $\langle \mathbf{X} \rangle$ denotes the the expectation value of $\mathbf{X}$. In [1] it was shown that the mean occupancy of the kth site at steady state is given by

$$\langle X_\mathbf{k} \rangle = \lambda/\mu_k. \tag{15}$$

The multidimensional probability generating function (PGF) of the occupancy vector was also studied in [1], and explicit steady-state PGFs were obtained for small ASIP systems ($n = 1, 2, 3$). This made clear that, similarly to the ASEP [7–10] and in contrast with other lattice gas models like the TJN and the related zero range process [50], PGFs in the ASIP do not admit a product form. In [1], an iterative algorithm that allows computation of steady-state PGFs for ASIP systems of arbitrary size was presented. However, explicit formulas for the PGFs of small ASIP systems are already very cumbersome and formulas for the PGFs of large ASIP systems are hard to obtain and virtually impossible to work with.

A little more is known about homogeneous ASIP systems [1,2]. In this subclass of ASIPs, all hopping rates are identical, $\mu = \mu_1 = \cdots = \mu_n$, and the marginals of the joint occupancy distribution at steady state can be computed exactly [30] and written in terms of Catalan numbers and their generalizations [51]. A formula for the factorial moments of the steady-state occupancies follows. Using this formula, it can be shown that the variance of the occupancy of the kth site is given by

$$\mathbf{Var}[X_\mathbf{k}] = \rho + \left(\frac{4\Gamma(k + 1/2)}{\sqrt{\pi}\,\Gamma(k)} - 1 \right)\rho^2, \tag{16}$$

where $\rho = \lambda/\mu$ is the mean site occupancy (also the average particle density) in the ASIP.

We derive Eq. (16) based on a known result for the factorial moments of X_k. In an homogeneous ASIP, the factorial moments are given by (Eq. (73) in Ref. [30])

$$\langle X_k(X_k - 1) \ldots (X_k - l + 1) \rangle$$
$$= \frac{2^l \rho^l \Gamma(1 + l/2)\Gamma(k + l/2 - 1/2)}{\sqrt{\pi}\,\Gamma(k)}, \tag{17}$$

where $k = 1, \ldots, n$ and $l = 1, 2, 3, \ldots$. In order to calculate the variance of X_k, we first calculate the first two factorial moments of X_k. Setting $l = 1$ in Eq. (17), we find

$$\langle X_k \rangle = \frac{2\rho\Gamma(3/2)\Gamma(k)}{\sqrt{\pi}\,\Gamma(k)} = \frac{2\rho\frac{\sqrt{\pi}}{2}}{\sqrt{\pi}} = \rho, \tag{18}$$

and setting $l = 2$ we find

$$\langle X_k(X_k - 1) \rangle = \frac{4\rho^2\Gamma(2)\Gamma(k + 1/2)}{\sqrt{\pi}\,\Gamma(k)} = \frac{4\rho^2\Gamma(k + 1/2)}{\sqrt{\pi}\,\Gamma(k)}. \tag{19}$$

Combining Eqs. (18) and (19), we see that the second moment is given by

$$\langle X_k^2 \rangle = \langle X_k \rangle + \langle X_k(X_k - 1) \rangle = \rho + \frac{4\rho^2\Gamma(k + 1/2)}{\sqrt{\pi}\,\Gamma(k)}. \tag{20}$$

The variance can now be obtained by combining Eqs. (18) and (20),

$$\mathbf{Var}[X_{\mathbf{k}}] = \langle X_{\mathbf{k}}^2 \rangle - \langle X_{\mathbf{k}} \rangle^2 = \rho + \left(\frac{4\Gamma(k+1/2)}{\sqrt{\pi}\,\Gamma(k)} - 1 \right)\rho^2,$$
(21)

which is identical to Eq. (16). In this paper, we generalize Eq. (16) to capture the full variance-covariance matrix of homogeneous and nonhomogeneous ASIPs at steady state.

F. The focus and structure of this paper

Occupancy correlations in the ASIP are captured by an n-dimensional variance-covariance matrix,

$$\mathbf{Cov}[\mathbf{X}(n,t)] \equiv \langle \mathbf{X}(n,t)\mathbf{X}(n,t)^\top \rangle - \langle \mathbf{X}(n,t) \rangle \langle \mathbf{X}(n,t)^\top \rangle,$$
(22)

in which the nondiagonal elements give the covariance between different sites, and the diagonal elements give the variances in the occupancy of sites. The remainder of the paper is dedicated to this variance-covariance matrix and is organized as follows. In Sec. II, we present a formula for the covariance matrix of a general ASIP at steady state. In addition, we give a closed-form expression for the covariance matrix of homogeneous ASIP systems of arbitrary size. The derivation of these results is given in Secs. III and IV, respectively. We conclude in Sec. V.

II. A SUMMARY OF KEY RESULTS ESTABLISHED IN THIS PAPER

In this section we present a short summary of the key results established in this paper. We give an exact formula for the occupancy correlation matrix of a general ASIP system at steady state and a closed-form expression for the correlation matrix of a homogeneous ASIP system at steady state. We start with some basic definitions and notation.

Throughout this paper we use the shorthand vector notation

$$\mathbf{e_{1,n}} = (1, 0, \ldots, 0)^\top \in \mathbb{R}^{n \times 1},$$
(23)

and the following set of linear operators $\mathbf{M_{k,n}} \in \mathbb{R}^{n \times n}$. The $\mathbf{M_{k,n}}$ operators represent the *change* in the occupancy vector that is caused due to the opening of the kth gate ($k = 1, \ldots, n$) in an ASIP system of n sites. The $\mathbf{M_{k,n}}$ operators operate on $\mathbf{X}(n,t)$ as

$$\mathbf{M_{1,n}}\mathbf{X}(n,t) = (-X_1(t), X_1(t), 0, \ldots, 0)^\top,$$
$$\mathbf{M_{2,n}}\mathbf{X}(n,t) = (0, -X_2(t), X_2(t), 0, \ldots, 0)^\top,$$
$$\vdots$$
$$\mathbf{M_{n-1,n}}\mathbf{X}(n,t) = (0, \ldots, 0, -X_{n-1}(t), X_{n-1}(t))^\top,$$
$$\mathbf{M_{n,n}}\mathbf{X}(n,t) = (0, \ldots, 0, -X_n(t))^\top$$
(24)

and have the matrix form

$$\mathbf{M_{k,n}}(i,j) = \begin{cases} -1, & k = i = j, \\ 1, & k = i - 1 = j, \\ 0 & \text{otherwise} \end{cases}$$
(25)

for $k < n$ and

$$\mathbf{M_{n,n}}(i,j) = \begin{cases} -1, & n = i = j, \\ 0 & \text{otherwise} \end{cases}$$
(26)

for $k = n$. In addition, we define the linear operator

$$\mathbf{P_n}\mathbf{X}(n,t) = (0, \ldots, 0, X_{n-1}(t))^\top \in \mathbb{R}^{n \times 1},$$
(27)

which will prove to be useful later.

With the aid of the above, we define an additional set of vectors and matrices: $\mathbf{V_k}$, $\mathbf{R_k}$, and $\mathbf{Q_k}$. We start with $\mathbf{V_k}$, which is defined as follows:

$$\mathbf{V_k} = \frac{\lambda^2}{\mu_k} \mathbf{e}_{\mathbf{1,k}}^\top \in \mathbb{R}^{1 \times k}.$$
(28)

We continue with $\mathbf{R_k}$, which is defined to be

$$\mathbf{R_k} = \sum_{i=1}^{k-1} \mu_i \mathbf{M_{i,k}}^\top + \mu_{k-1}\mathbf{P_k}^\top - \mu_k \mathbf{I},$$
(29)

where μ_i is the gate opening rate of the ith gate, the matrices $\mathbf{M_{i,k}}$ are defined in Eq. (25), the matrix $\mathbf{P_k}$ is defined in Eq. (27), and $\mathbf{I}$ stands for the identity matrix. We observe that $\mathbf{R_k}$ is an upper triangular matrix of the form

$$\mathbf{R_k} = \begin{pmatrix} -\mu_1 - \mu_k & \mu_1 & & & \\ & -\mu_2 - \mu_k & \ddots & & \\ & & \ddots & \mu_{k-2} & \\ & & & -\mu_{k-1} - \mu_k & 2\mu_{k-1} \\ & & & & -\mu_k \end{pmatrix}$$
$$\in \mathbb{R}^{k \times k},$$
(30)

which, in particular, means that the inverse $\mathbf{R_k^{-1}}$ exists and is also an upper triangular matrix. Finally, we define $\mathbf{Q_2} = (0, \quad \mu_1)$ and

$$\mathbf{Q_k} = \begin{pmatrix} \mu_{k-1} & & \cdots & & \\ & \mu_{k-1} & & & \\ \vdots & & \ddots & & \\ & & & \mu_{k-1} & \vdots \\ & & \cdots & 0 & \mu_{k-1} \end{pmatrix} \in \mathbb{R}^{(k-1) \times k}$$
(31)

for $k > 2$. Here, and in all of the above matrices, blank spaces represent 0 entries.

We are now ready to state the main results of this paper. The covariance matrix of the occupancy vector $\mathbf{X}(n)$ is an $n \times n$ symmetric matrix that is given by

$$\mathbf{Cov}[\mathbf{X}(n)] \equiv \langle \mathbf{X}(n)\mathbf{X}(n)^\top \rangle - \langle \mathbf{X}(n) \rangle \langle \mathbf{X}(n)^\top \rangle.$$
(32)

The second term in Eq. (32) can be easily obtained from Eq. (15) and is given by

$$(\langle \mathbf{X}(n) \rangle \langle \mathbf{X}(n)^\top \rangle)_{i,j} = \frac{\lambda^2}{\mu_i \mu_j}.$$
(33)

The first term in Eq. (32) is the cross-correlation matrix $\langle \mathbf{X}(n)\mathbf{X}(n)^\top \rangle$. In Sec. III, we show that the rows of this matrix admit a recursion relation which allows their computation (Fig. 1). We start by showing that

$$\langle X_1 X_1 \rangle = \langle X_1^2 \rangle = \frac{\lambda(2\lambda + \mu_1)}{\mu_1^2}$$
(34)

and that

$$\langle X_2 \mathbf{X}^\top(2) \rangle = -\mathbf{V_2}\mathbf{R_2^{-1}} - \langle X_1 X_1 \rangle \mathbf{Q_2}\mathbf{R_2^{-1}}$$
(35)

$$\begin{pmatrix} \langle X_1 X_1 \rangle & & \\ & & \\ & & \end{pmatrix} \Longrightarrow \begin{pmatrix} \langle X_1 X_1 \rangle & & \\ \langle X_2 X_1 \rangle & \langle X_2 X_2 \rangle & \\ & & \end{pmatrix} \Longrightarrow \begin{pmatrix} \langle X_1 X_1 \rangle & & \\ \langle X_2 X_1 \rangle & \langle X_2 X_2 \rangle & \\ \langle X_3 X_1 \rangle & \langle X_3 X_2 \rangle & \langle X_3 X_3 \rangle \end{pmatrix}$$

FIG. 1. In Sec. III, we show that the rows of the cross-correlation matrix obey a recursive relation. Given $\langle X_1 X_1 \rangle$ one can compute $\langle X_2 X_1 \rangle$ and $\langle X_2 X_2 \rangle$. Then, given $\langle X_2 X_1 \rangle$ and $\langle X_2 X_2 \rangle$, one can compute $\langle X_3 X_1 \rangle$, $\langle X_3 X_2 \rangle$, and $\langle X_3 X_3 \rangle$. Proceeding in this way one can obtain the lower triangular half of $\langle \mathbf{X}(n)\mathbf{X}(n)^\top \rangle$ and, by symmetry, the entire matrix.

and, from there, continue to show that for $k \geqslant 3$, the kth row of the lower triangular half of the cross-correlation matrix is given by

$$\langle X_k \mathbf{X}^\top(k) \rangle = -\mathbf{V_k R_k^{-1}} + \sum_{i=2}^{k-1} (-1)^{k-i+1} \mathbf{V_i R_i^{-1}} \prod_{j=i+1}^{k} \mathbf{Q_j R_j^{-1}}$$

$$+ (-1)^{k-1} \frac{\lambda(2\lambda + \mu_1)}{\mu_1^2} \prod_{i=2}^{k} \mathbf{Q_i R_i^{-1}}. \qquad (36)$$

The full matrix can then be obtained by reflecting the entries of the lower triangular matrix about its main diagonal.

In Fig. 2, we graphically demonstrate various aspects of the result in Eq. (36). We do this with an ASIP of $n = 100$ sites in which $\lambda = 1$ and the μ_k's are taken to be the first 100 nonzero digits of the number π. First, we compare our analytical result with numerical simulations [Figs. 2(a)–2(c)]. We observe that correlations in the ASIP model drop rapidly with the distance between sites, which in turn requires high-precision simulations. Indeed, even when sampling 10^6 steady-state occupancy vectors, reliable estimates could only be obtained for the covariance of the first site with its four consecutive sites [Fig. 2(a)], and increasing the number of samples to 10^7 and 10^8 was only able to increase reliable estimates to six and eight consecutive sites, respectively. In their range of validity, numerical simulations agree well with Eq. (36), but the hardship involved in extending this range also makes it clear that long-distance correlations in the ASIP can only be obtained analytically. Figures 2(d) and 2(e) show that long-distance correlations can be easily obtained using Eq. (36).

We now describe occupancy correlations in homogeneous ASIPs for which all gate opening rates are equal: $\mu = \mu_1 = \cdots = \mu_n$. In Sec. III, we show that in this case the result in
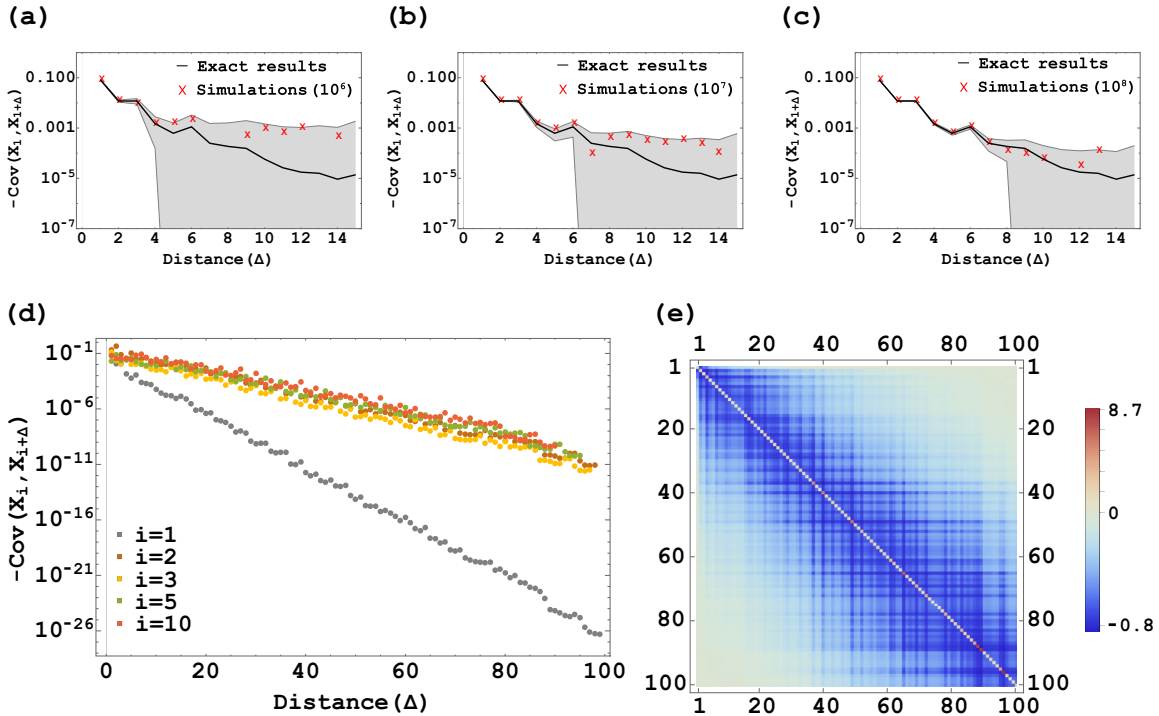

FIG. 2. Numerical validation and graphical illustration of the result in Eq. (36). (a)–(c) Comparison with numerical simulations. The exact result for the covariance between X_1 and $X_{1+\Delta}$ is plotted vs the distance Δ between the two sites (solid black line). Note that the covariance is always negative and that it quickly drops with the distance. Results from simulations are presented as red crosses. These were obtained by sampling 10^6 (a), 10^7 (b), and 10^8 (c) occupancy vectors. One can observe that the uncertainty around the numerical estimates (shaded gray) slowly diminishes as the number of samples increases, thus converging to the black theory line. However, it is also clear that obtaining numerical estimates for the correlation between sites that are far apart is virtually impossible in the ASIP, as this would typically require a huge number of samples which cannot be obtained in a reasonable time. This emphasizes the importance of exact solutions. (d) The exact result for the covariance between X_i and $X_{i+\Delta}$ is plotted as a function of the distance Δ for $i = 1, 2, 3, 5$, and 10. As expected, correlations generally become weaker with distance, but now one can also observe that the decay is approximately exponential. (e) Heat map representation of the covariance matrix $\langle \mathbf{X}(n)\mathbf{X}(n)^\top \rangle$. Correlations are color coded: deep red or blue represents a strong positive or negative correlation, respectively, and white represents a weak correlation.
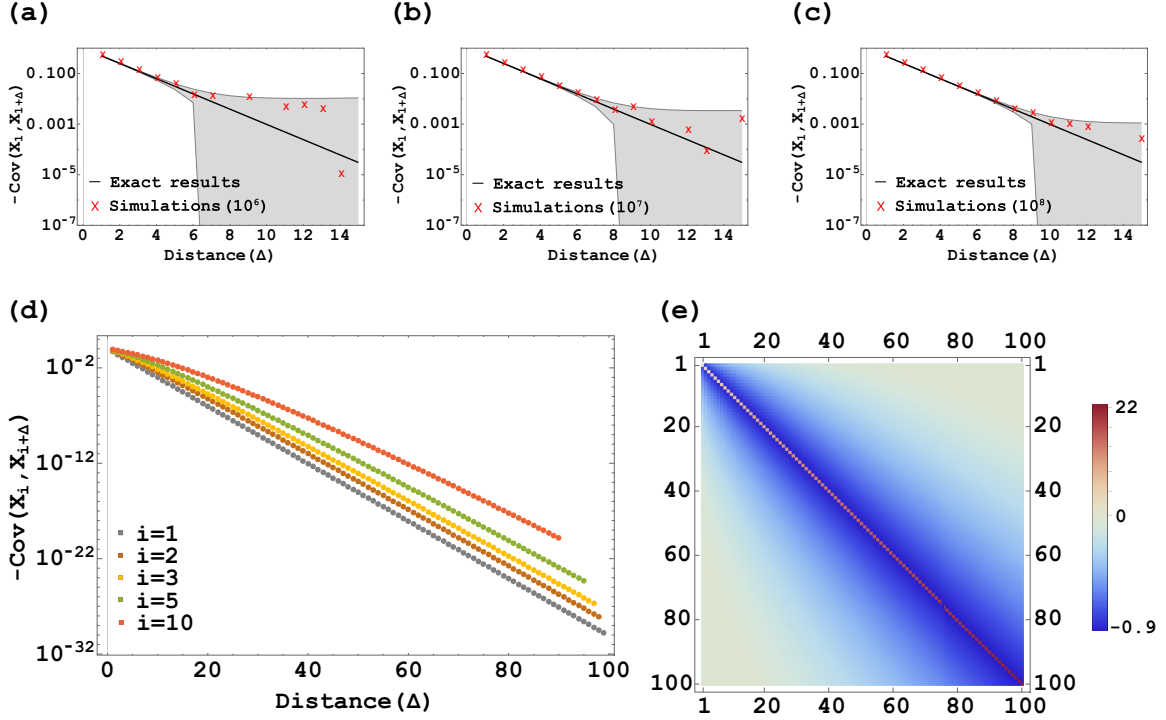
FIG. 3. Numerical validation and graphical illustration of the result in Eq. (37). Here, $n = 100$ and $\lambda = \mu_1 = \cdots = \mu_n = 1$. (a)–(c) Comparison with numerical simulations. The exact result for the covariance between X_1 and $X_{1+\Delta}$ is plotted vs the distance Δ between the two sites (solid black line). Note that the covariance is always negative and that it quickly drops with the distance. Results from simulations are presented as red crosses. These were obtained by sampling 10^6 (a), 10^7 (b), and 10^8 (c) occupancy vectors. One can observe that the uncertainty around the numerical estimates (shaded gray) slowly diminishes as the number of samples increases, thus converging to the black theory line. (d) The exact result for the covariance between X_i and $X_{i+\Delta}$ is plotted as a function of the distance Δ for values of $i = 1, 2, 3, 5$, and 10. As expected, correlations generally become weaker with distance, but now one can also observe that the decay is approximately exponential. (e) Heat map representation of the covariance matrix $\langle \mathbf{X}(n)\mathbf{X}(n)^\top \rangle$. Correlations are color coded: deep red or blue represents a strong positive or negative correlation, respectively, and white represents a weak correlation.

Eq. (36) can be simplified to give

$$(\mathbf{Cov}[\mathbf{X}(n)])_{i,j} = \begin{cases} \left(\frac{1}{2^{i+j-1}}\binom{j+i-1}{\min(i,\,j)}\,{}_2F_1\left(1, i+j, 1+\min(i,j); \frac{1}{2}\right) - 2\right)\rho^2, & i \neq j, \\[2mm] \rho + \left(\frac{4\Gamma(i+1/2)}{\sqrt{\pi}\,\Gamma(i)} - 1\right)\rho^2, & i = j, \end{cases} \tag{37}$$

where ${}_2F_1(a, b, c; x)$ is the hypergeometric function, $\Gamma(x)$ is the gamma function, and $\rho = \lambda/\mu$ is the mean site occupancy. An interesting property of Eq. (37) is its invariance with respect to a change of time scale: the covariance matrix of a homogeneous ASIP with rates λ and μ is identical to the covariance matrix of a homogeneous ASIP with rates $\alpha\lambda$ and $\alpha\mu$ ($\alpha > 0$). In Sec. III, we show that this is also true for inhomogeneous ASIP systems. The derivation of Eq. (37) is carried out in Sec. III. For numerical validation and graphical illustration of this result see Fig. 3.

III. CORRELATION MATRIX: EXACT RESULTS

In this section, we derive and solve an equation for the cross-correlation matrix of an ASIP at steady state.

A. Temporal dynamics of the cross-correlation matrix

We start by deriving an equation for the temporal dynamics of the cross-correlation matrix $\langle \mathbf{X}(n, t)\mathbf{X}^\top(n, t)\rangle$. Consider an ASIP of n sites and observe the system at times t and $t' = t + \Delta$ (for small Δ). We would like to find a relation between the cross-correlation matrices $\langle \mathbf{X}(n, t')\mathbf{X}^\top(n, t')\rangle$ and $\langle \mathbf{X}(n, t)\mathbf{X}^\top(n, t)\rangle$. To do so, we rewrite the Markovian law of motion in

Eq. (14) as

$$
\mathbf{X}(n, t') = \begin{cases}
\mathbf{X}(n, t) & \text{w.p.} \quad 1 - (\lambda + \mu_c)\Delta + o(\Delta), \\[6pt]
\mathbf{X}(n, t) + \mathbf{e_{1,n}} & \text{w.p.} \quad \lambda\Delta + o(\Delta), \\[6pt]
\mathbf{X}(n, t) + \mathbf{M_{1,n}}\mathbf{X}(n, t) & \text{w.p.} \quad \mu_1\Delta + o(\Delta), \\[6pt]
\mathbf{X}(n, t) + \mathbf{M_{2,n}}\mathbf{X}(n, t) & \text{w.p.} \quad \mu_2\Delta + o(\Delta), \\[6pt]
\vdots & \qquad \vdots \\[6pt]
\mathbf{X}(n, t) + \mathbf{M_{n-1,n}}\mathbf{X}(n, t) & \text{w.p.} \quad \mu_{n-1}\Delta + o(\Delta), \\[6pt]
\mathbf{X}(n, t) + \mathbf{M_{n,n}}\mathbf{X}(n, t) & \text{w.p.} \quad \mu_n\Delta + o(\Delta),
\end{cases}
\tag{38}
$$

where the vector $\mathbf{e_{1,n}}$ and the operators $\mathbf{M_{k,n}}$ are defined in Eqs. (23) and (24), respectively. Now, we utilize the law of total expectation to obtain

$$
\langle \mathbf{X}(n, t')\mathbf{X}^\top(n, t') \rangle = \begin{cases}
(1 - (\lambda + \mu_c)\Delta)\langle \mathbf{X}(n, t)\mathbf{X}^\top(n, t) \rangle \\
+ \\
\lambda\Delta\langle (\mathbf{X}(n, t) + \mathbf{e_{1,n}})(\mathbf{X}(n, t) + \mathbf{e_{1,n}})^\top \rangle \\
+ \\
\mu_1\Delta\langle (\mathbf{X}(n, t) + \mathbf{M_{1,n}}\mathbf{X}(n, t))(\mathbf{X}(n, t) + \mathbf{M_{1,n}}\mathbf{X}(n, t))^\top \rangle \\
+ \\
\mu_2\Delta\langle (\mathbf{X}(n, t) + \mathbf{M_{2,n}}\mathbf{X}(n, t))(\mathbf{X}(n, t) + \mathbf{M_{2,n}}\mathbf{X}(n, t))^\top \rangle \\
+ \cdots + \\
\mu_{n-1}\Delta\langle (\mathbf{X}(n, t) + \mathbf{M_{n-1,n}}\mathbf{X}(n, t))(\mathbf{X}(n, t) + \mathbf{M_{n-1,n}}\mathbf{X}(n, t))^\top \rangle \\
+ \\
\mu_n\Delta\langle (\mathbf{X}(n, t) + \mathbf{M_{n,n}}\mathbf{X}(n, t))(\mathbf{X}(n, t) + \mathbf{M_{n,n}}\mathbf{X}(n, t))^\top \rangle \\
+ \\
o(\Delta),
\end{cases}
\tag{39}
$$

where we recall that $\mu_c = \mu_1 + \cdots + \mu_n$.

Rearranging terms in Eq. (39), dividing by Δ, and taking $\Delta \to 0$, we find that

$$
\frac{d\langle \mathbf{X}(n, t)\mathbf{X}^\top(n, t) \rangle}{dt} = \begin{cases}
\lambda[\langle \mathbf{X}(n, t) \rangle \mathbf{e_{1,n}^\top} + \mathbf{e_{1,n}}\langle \mathbf{X}(n, t)^\top \rangle + \mathbf{e_{1,n}}\mathbf{e_{1,n}^\top}] \\
+ \\
\langle \mathbf{X}(n, t)\mathbf{X}^\top(n, t) \rangle \left(\sum_{i=1}^n \mu_i \mathbf{M_{i,n}} \right)^\top \\
+ \\
\left(\sum_{i=1}^n \mu_i \mathbf{M_{i,n}} \right)\langle \mathbf{X}(n, t)\mathbf{X}^\top(n, t) \rangle \\
+ \\
\sum_{i=1}^n \mu_i \mathbf{M_{i,n}}\langle \mathbf{X}(n, t)\mathbf{X}^\top(n, t) \rangle \mathbf{M_{i,n}^\top}.
\end{cases}
\tag{40}
$$

Equation (40) governs the temporal dynamics of the cross-correlation matrix $\langle \mathbf{X}(n, t)\mathbf{X}^\top(n, t) \rangle$ in the ASIP. In what follows, we also specifically require $\langle \mathbf{X}_n(t)\mathbf{X}^\top(n, t) \rangle$, i.e., the last row in the cross-correlation matrix $\langle \mathbf{X}(n, t)\mathbf{X}^\top(n, t) \rangle$. Equation (40) can be used to write an equation for $\langle \mathbf{X}_n(t)\mathbf{X}^\top(n, t) \rangle$, but it is actually easier to derive this equation from scratch.

Consider the same ASIP system as before and observe it at times t and $t' = t + \Delta$ (for small Δ). Following the same recipe that led to Eq. (39), we find that the relation between $\langle X_n(t') \mathbf{X}^\top(n, t') \rangle$ and $\langle X_n(t) \mathbf{X}^\top(n, t) \rangle$ is given by

$$\langle X_n(t') \mathbf{X}^\top(n, t') \rangle = \begin{cases} (1 - (\lambda + \mu_c)\Delta)\langle X_n(t)\mathbf{X}^\top(n, t)\rangle \\ + \\ \lambda\Delta\langle X_n(t)(\mathbf{X}(n, t) + \mathbf{e_{1,n}})^\top\rangle \\ + \\ \mu_1\Delta\langle X_n(t)(\mathbf{X}(n, t) + \mathbf{M_{1,n}}\mathbf{X}(n, t))^\top\rangle \\ + \\ \mu_2\Delta\langle X_n(t)(\mathbf{X}(n, t) + \mathbf{M_{2,n}}\mathbf{X}(n, t))^\top\rangle \\ + \cdots + \\ \mu_{n-1}\Delta\langle (X_n(t) + X_{n-1}(t))(\mathbf{X}(n, t) + \mathbf{M_{n-1,n}}\mathbf{X}(n, t))^\top\rangle \\ + \\ \mu_n\Delta\langle 0 \cdot (\mathbf{X}(n, t) + \mathbf{M_{n,n}}\mathbf{X}(n, t))^\top\rangle \\ + \\ o(\Delta). \end{cases} \quad (41)$$

Rearranging terms in Eq. (41), dividing by Δ, and taking $\Delta \to 0$, we find

$$\frac{d\langle X_n(t)\mathbf{X}^\top(n, t)\rangle}{dt} = \begin{cases} \lambda\langle X_n(t)\rangle \mathbf{e_{1,n}^\top} \\ + \\ \langle X_n(t)\mathbf{X}^\top(n, t)\rangle \left[\sum_{i=1}^{n-1}\mu_i \mathbf{M_{i,n}^\top} - \mu_n \mathbf{I}\right] \\ + \\ \mu_{n-1}\langle X_{n-1}\mathbf{X}^\top(n, t)\rangle[\mathbf{M_{n-1,n}^\top} + \mathbf{I}]. \end{cases} \quad (42)$$

B. Steady state

In this subsection, we derive an explicit steady-state solution for Eq. (40). We do so in several steps. In the first step, we establish a recursion relation by finding the steady-state solution for $\langle X_n(t)\mathbf{X}^\top(n, t)\rangle$ in Eq. (42) and showing that it can be written in terms of the steady-state solution for $\langle X_{n-1}(t)\mathbf{X}^\top(n-1, t)\rangle$, i.e., the last row in the cross-correlation matrix of an ASIP that lacks the nth site. We start by noting that at steady state Eq. (42) reduces to

$$0 = \begin{cases} \lambda^2 \mathbf{e_{1,n}^\top}/\mu_n \\ + \\ \langle X_n\mathbf{X}^\top(n)\rangle\left[\sum_{i=1}^{n-1}\mu_i\mathbf{M_{i,n}^\top} - \mu_n\mathbf{I}\right] \\ + \\ \mu_{n-1}\langle X_{n-1}\mathbf{X}^\top(n)\rangle[\mathbf{M_{n-1,n}^\top} + \mathbf{I}], \end{cases} \quad (43)$$

where we have used $\langle X_n \rangle = \lambda/\mu_n$ [Eq. (15)]. In order to proceed, we simplify $\langle X_{n-1}\mathbf{X}^\top(n)\rangle$, which appears in the bottom row of Eq. (43). To this end, we make use of the "embedding" property of the ASIP [1].

The embedding property is described as follows. Consider two ASIP systems, (A) and (B), and set the number of sites in these systems to n_A and n_B, respectively, where $n_A \leqslant n_B$. Assume that the inflow rate λ and the opening rates of the first n_A gates are identical in systems (A) and (B). It can then be shown that the steady-state occupancy of model system (A) is statistically identical to the steady-state occupancy of the first n_A sites of model system (B). In other words, system (A) will have the same steady state when it stands alone and when it is embedded within system (B) [as long as the embedding is done in the manner described above]. To intuitively understand the embedding property one simply needs to realize that a part of an ASIP system cannot feed back on a disjoint part of the system which is located upstream with respect to it (closer to the first site). Thus, the steady-state distribution of the first n_A sites in system (B) cannot depend on the remaining $n_B - n_A$ sites that are located downstream to it. A formal proof of the embedding property is given in Ref. [1].

The embedding property of the ASIP implies that the steady-state occupancy distribution of the first $n - 1$ sites in an ASIP of n sites are identical to the steady-state occupancy distribution in an ASIP of $n - 1$ sites that has the same inflow and gate opening rates. Using this, we can write $\langle X_{n-1}\mathbf{X}^\top(n)\rangle$, which appears on the right-hand side of Eq. (43) as

$$\langle X_{n-1}\mathbf{X}^\top(n)\rangle = (\langle X_{n-1}\mathbf{X}^\top(n-1)\rangle, 0) \\ + (0, \ldots, 0, \langle X_{n-1}X_n\rangle), \quad (44)$$

and further note that

$$\langle X_{n-1}\mathbf{X}^\top(n)\rangle = (\langle X_{n-1}\mathbf{X}^\top(n-1)\rangle, 0) + (\mathbf{P_n}\langle X_n\mathbf{X}(n)\rangle)^\top, \quad (45)$$

where we have used the operator $\mathbf{P_n}$ defined in Eq. (27). Substituting Eq. (45) into Eq. (43), noting that

$$(\mathbf{P_n}\langle X_n\mathbf{X}(n)\rangle)^\top\mathbf{M_{n-1,n}^\top} = (\mathbf{M_{n-1,n}}(0, \ldots, 0, \langle X_{n-1}X_n\rangle))^\top \\ = \mathbf{0}, \quad (46)$$

and rearranging yields the recursion relation

$$\langle X_n\mathbf{X}^\top(n)\rangle = -\left[\frac{\lambda^2}{\mu_n}\mathbf{e_{1,n}^\top} + \mu_{n-1}(\langle X_{n-1}\mathbf{X}^\top(n-1)\rangle, 0)\right. \\ \left. \times [\mathbf{M_{n-1,n}^\top} + \mathbf{I}]\right]\mathbf{R_n^{-1}}, \quad (47)$$

where the matrix $\mathbf{R_n}$ is defined in Eq. (29). Equation (47) connects $\langle X_n\mathbf{X}^\top(n)\rangle$ with $\langle X_{n-1}\mathbf{X}^\top(n-1)\rangle$ and thus provides an iterative method for computing the cross-correlation matrix.

For $n > 2$, Eq. (47) can be further simplified. In order to do so, we utilize the embedding property one more time to obtain

$$\langle X_n \mathbf{X}^\top(n) \rangle = -\left[\frac{\lambda^2}{\mu_n} \mathbf{e}_{\mathbf{1,n}}^\top + \mu_{n-1}(\langle X_{n-1} \mathbf{X}^\top(n-2) \rangle, \right.$$

$$\left. \langle X_{n-1} X_{n-1} \rangle, 0) \left[\mathbf{M}_{\mathbf{n-1,n}}^\top + \mathbf{I} \right] \right] \mathbf{R}_{\mathbf{n}}^{-1}. \quad (48)$$

Noting that (for $n \geqslant 2$)

$$\mathbf{M}_{\mathbf{n-1,n}}^\top + \mathbf{I} = \begin{pmatrix} 1 & & & & 0 \\ & \ddots & & & 0 \\ & & 1 & \vdots \\ & & \cdots & 0 & 1 \\ & & \cdots & 0 & 1 \end{pmatrix}, \quad (49)$$

and taking the vector-matrix product in parentheses in Eq. (48) we find

$$\langle X_n \mathbf{X}^\top(n) \rangle = -\left[\frac{\lambda^2}{\mu_n} \mathbf{e}_{\mathbf{1,n}}^\top + \mu_{n-1}(\langle X_{n-1} \mathbf{X}^\top(n-2) \rangle, 0, \right.$$

$$\left. \langle X_{n-1} X_{n-1} \rangle) \right] \mathbf{R}_{\mathbf{n}}^{-1}. \quad (50)$$

Finally, noting that

$$\mu_{n-1}(\langle X_{n-1} \mathbf{X}(n-2) \rangle^\top, 0, \langle X_{n-1} X_{n-1} \rangle)$$

$$= \langle X_{n-1} \mathbf{X}(n-1)^\top \rangle \mathbf{Q}_{\mathbf{n}}, \quad (51)$$

where $\mathbf{Q}_{\mathbf{n}}$ is defined in Eq. (31), we conclude that

$$\langle X_n \mathbf{X}^\top(n) \rangle = -\mathbf{V}_{\mathbf{n}} \mathbf{R}_{\mathbf{n}}^{-1} - \langle X_{n-1} \mathbf{X}^\top(n-1) \rangle \mathbf{Q}_{\mathbf{n}} \mathbf{R}_{\mathbf{n}}^{-1}, \quad (52)$$

where $\mathbf{V}_{\mathbf{n}}$ is defined in Eq. (28). Applying the iteration in Eq. (52) time and again one can solve for the cross-correlation matrix of an arbitrary ASIP system of size $n > 2$. The base for these iterations (seed) is the cross-correlation matrix of an ASIP system of size $n = 2$, which we now compute. The cross-correlation matrix of an ASIP system of size $n = 1$ is also obtained as a preliminary step.

In order to obtain a steady-state solution for an ASIP system of size $n = 1$ we substitute Eqs. (23), (25), and (26) into Eq. (40) and set the left-hand side of this equation to 0. This gives

$$0 = \lambda(2\langle X_1 \rangle + 1) - \mu_1 \langle X_1^2 \rangle - \mu_1 \langle X_1^2 \rangle + \mu_1 \langle X_1^2 \rangle. \quad (53)$$

Equation (53) can be solved by substituting $\langle X_1 \rangle = \lambda/\mu_1$ [Eq. (15)], and rearranging terms gives

$$\langle X_1^2 \rangle = \frac{\lambda(2\lambda + \mu_1)}{\mu_1^2}. \quad (54)$$

We note in passing that this result can also be obtained by utilizing the fact that the occupancy of an ASIP system with a single site comes from the geometric distribution [1].

The solution for $n = 2$, $\langle X_2 \mathbf{X}^\top(2) \rangle$, can be obtained by solving Eq. (47) for $n = 2$. To do so, we start by calculating $\mathbf{R}_2$ [Eq. (29)]:

$$\mathbf{R}_2 = \mu_1 \mathbf{M}_{\mathbf{1,2}}^\top + \mu_1 \mathbf{P}_{\mathbf{2}}^\top - \mu_2 \mathbf{I} = \begin{pmatrix} -\mu_1 - \mu_2 & 2\mu_1 \\ 0 & -\mu_2 \end{pmatrix}. \quad (55)$$

Now, we observe that $\mathbf{R}_2^{-1}$ is given by

$$\mathbf{R}_2^{-1} = \begin{pmatrix} \frac{-1}{\mu_1+\mu_2} & \frac{-2\mu_1}{\mu_2(\mu_1+\mu_2)} \\ 0 & \frac{-1}{\mu_2} \end{pmatrix}. \quad (56)$$

Substituting Eqs. (23), (25), and (56) into Eq. (47) then yields

$$\langle X_2 \mathbf{X}^\top(2) \rangle$$

$$= -\left[\frac{\lambda^2}{\mu_2}(1, \ 0) + \mu_1(\langle X_1 X_1 \rangle, \ 0) \right.$$

$$\left. \times \left[\begin{pmatrix} -1 & 1 \\ 0 & 0 \end{pmatrix} + \begin{pmatrix} 1 & 0 \\ 0 & 1 \end{pmatrix} \right] \right] \begin{pmatrix} \frac{-1}{\mu_1+\mu_2} & \frac{-2\mu_1}{\mu_2(\mu_1+\mu_2)} \\ 0 & -\frac{1}{\mu_2} \end{pmatrix}.$$

$$(57)$$

Substituting Eq. (54) into Eq. (57) we find

$$\langle X_2 \mathbf{X}^\top(2) \rangle = \left(\frac{\lambda^2}{\mu_2(\mu_1+\mu_2)}, \frac{2\mu_1\lambda^2}{\mu_2^2(\mu_1+\mu_2)} + \frac{\lambda(2\lambda+\mu_1)}{\mu_1\mu_2} \right),$$

$$(58)$$

which can be brought into the form of Eq. (52) by noting that

$$\langle X_2 \mathbf{X}^\top(2) \rangle = -\mathbf{V}_2 \mathbf{R}_2^{-1} - \frac{\lambda(2\lambda+\mu_1)}{\mu_1^2} \mathbf{Q}_2 \mathbf{R}_2^{-1}, \quad (59)$$

with $\mathbf{Q}_2 = (0, \ \mu_1)$.

Solutions for ASIP systems with $n > 2$ can now be obtained in terms of $\mathbf{V}_{\mathbf{n}}$, $\mathbf{R}_{\mathbf{n}}$, and $\mathbf{Q}_{\mathbf{n}}$ by substituting Eq. (59) into Eq. (52) and progressing iteratively. Doing this, we find

$$\langle X_3 \mathbf{X}^\top(3) \rangle = -\mathbf{V}_3 \mathbf{R}_3^{-1} + \mathbf{V}_2 \mathbf{R}_2^{-1} \mathbf{Q}_3 \mathbf{R}_3^{-1}$$

$$+ \frac{\lambda(2\lambda+\mu_1)}{\mu_1^2} \mathbf{Q}_2 \mathbf{R}_2^{-1} \mathbf{Q}_3 \mathbf{R}_3^{-1},$$

$$\langle X_4 \mathbf{X}^\top(4) \rangle = -\mathbf{V}_4 \mathbf{R}_4^{-1} + \mathbf{V}_3 \mathbf{R}_3^{-1} \mathbf{Q}_4 \mathbf{R}_4^{-1}$$

$$- \mathbf{V}_2 \mathbf{R}_2^{-1} \mathbf{Q}_3 \mathbf{R}_3^{-1} \mathbf{Q}_4 \mathbf{R}_4^{-1}$$

$$- \frac{\lambda(2\lambda+\mu_1)}{\mu_1^2} \mathbf{Q}_2 \mathbf{R}_2^{-1} \mathbf{Q}_3 \mathbf{R}_3^{-1} \mathbf{Q}_4 \mathbf{R}_4^{-1}. \quad (60)$$

Continuing in a similar fashion, we obtain the general formula in Eq. (36).

An interesting property of the covariance matrix of the ASIP at steady state is its invariance with respect to a change of time scale. Consider an ASIP system (A) with n sites and parameters $\{\lambda, \mu_1, \mu_2, \ldots, \mu_n\}$ and an ASIP system (B) with n sites and parameters $\{\alpha\lambda, \alpha\mu_1, \alpha\mu_2, \ldots, \alpha\mu_n\}$, where $\alpha > 0$ is a nonzero scalar. Substituting the rates of both systems into Eqs. (28), (29), and (31) yields

$$\mathbf{R}_n^B = \alpha \mathbf{R}_{\mathbf{n}}^A,$$

$$\left(\mathbf{R}_{\mathbf{n}}^B \right)^{-1} = \frac{1}{\alpha} \left(\mathbf{R}_{\mathbf{n}}^A \right)^{-1},$$

$$\mathbf{Q}_{\mathbf{n}}^B = \alpha \mathbf{Q}_{\mathbf{n}}^A,$$

$$\mathbf{V}_{\mathbf{n}}^B = \alpha \mathbf{V}_{\mathbf{n}}^A. \quad (61)$$

Substituting Eq. (61) into Eq. (36) and applying the algorithm illustrated in Fig. 1, we obtain that the cross-correlation matrices of systems (A) and (B) are identical. In addition, it is easy to see that Eq. (33) yields the same result for both systems. These results, together with Eq. (32), prove invariance with respect to a change of time scale.

IV. CORRELATION MATRIX: HOMOGENEOUS SYSTEMS

In Sec. III, we have presented results for general ASIPs. In this section, we restrict ourselves to the case of homogeneous ASIPs, i.e., systems in which all gate opening rates are identical. For these ASIPs, we present a simple formula for the covariance matrix and discuss its special properties. We start by writing explicit expressions for the vector-matrix and matrix-matrix products which appear in Eq. (36).

Consider a homogeneous ASIP where $\mu = \mu_1 = \cdots = \mu_n$. Equation (30) then reduces to

$$\mathbf{R_n} = \begin{pmatrix} -2\mu & \mu & & & \\ & -2\mu & \ddots & & \\ & & \ddots & \mu & \\ & & & -2\mu & 2\mu \\ & & & & -\mu \end{pmatrix}, \quad (62)$$

and the inverse matrix, $\mathbf{R_n^{-1}}$, is then given by

$$\mathbf{R_n^{-1}} = \begin{pmatrix} -\frac{1}{2\mu} & -\frac{1}{4\mu} & \cdots & -\frac{1}{2^{n-2}\mu} & -\frac{1}{2^{n-1}\mu} & -\frac{1}{2^{n-2}\mu} \\ & -\frac{1}{2\mu} & \cdots & -\frac{1}{2^{n-3}\mu} & -\frac{1}{2^{n-2}\mu} & -\frac{1}{2^{n-3}\mu} \\ & & \ddots & \vdots & \vdots & \vdots \\ & & & -\frac{1}{4\mu} & & -\frac{1}{2\mu} \\ & & & & -\frac{1}{2\mu} & -\frac{1}{\mu} \\ & & & & & -\frac{1}{\mu} \end{pmatrix}. \quad (63)$$

Now, using the definition of $\mathbf{V_i}$ in Eq. (28), we compute $\mathbf{V_i R_i^{-1}}$ and find

$$\mathbf{V_2 R_2^{-1}} = -\left(\frac{\lambda}{\mu}\right)^2 \left(\frac{1}{2}, \; 1\right) \quad (64)$$

for $i = 2$ and

$$\mathbf{V_i R_i^{-1}} = -\left(\frac{\lambda}{\mu}\right)^2 \left(\frac{1}{2}, \; \frac{1}{4}, \; \cdots, \; \frac{1}{2^{i-1}}, \; \frac{1}{2^{i-2}}\right) \quad (65)$$

for $i > 2$. Similarly, using the definition of $\mathbf{Q_i}$ given in Eq. (31) and above it, we compute $\mathbf{Q_i R_i^{-1}}$ and find

$$\mathbf{Q_2 R_2^{-1}} = (0, \; -1) \quad (66)$$

for $i = 2$ and

$$\mathbf{Q_i R_i^{-1}} = \begin{pmatrix} -\frac{1}{2} & -\frac{1}{4} & \cdots & -\frac{1}{2^{i-2}} & -\frac{1}{2^{i-1}} & -\frac{1}{2^{i-2}} \\ 0 & -\frac{1}{2} & \cdots & \frac{1}{2^{i-3}} & -\frac{1}{2^{i-2}} & -\frac{1}{2^{i-3}} \\ 0 & 0 & \ddots & \vdots & \vdots & \vdots \\ 0 & 0 & 0 & -\frac{1}{2} & -\frac{1}{4} & -\frac{1}{2} \\ 0 & 0 & 0 & 0 & 0 & -1 \end{pmatrix} \quad (67)$$

for $i > 2$.

Evaluating the cross-correlation matrix $\langle \mathbf{X}(n)\mathbf{X}(n)^\top \rangle$ of a homogeneous ASIP system of arbitrary size can be done by substituting Eqs. (63)–(67) back into Eq. (36) and carrying out the computation using a standard computer algebra software. The covariance matrix then follows immediately and reveals a striking regularity. To demonstrate it, we consider a homogeneous ASIP with six sites. Setting $\rho = \lambda/\mu$, we find that the covariance matrix for this system is given by

$$\mathbf{Cov}[\mathbf{X}(6)] = \begin{pmatrix} \rho^2 + \rho & -\frac{1}{2}\rho^2 & -\frac{1}{4}\rho^2 & -\frac{1}{8}\rho^2 & -\frac{1}{16}\rho^2 & -\frac{1}{32}\rho^2 \\ -\frac{1}{2}\rho^2 & 2\rho^2 + \rho & -\frac{5}{8}\rho^2 & -\frac{6}{16}\rho^2 & -\frac{7}{32}\rho^2 & -\frac{8}{64}\rho^2 \\ -\frac{1}{4}\rho^2 & -\frac{5}{8}\rho^2 & \frac{11}{4}\rho^2 + \rho & -\frac{22}{32}\rho^2 & -\frac{29}{64}\rho^2 & -\frac{37}{128}\rho^2 \\ -\frac{1}{8}\rho^2 & -\frac{6}{16}\rho^2 & -\frac{22}{32}\rho^2 & \frac{27}{8}\rho^2 + \rho & -\frac{93}{128}\rho^2 & -\frac{130}{256}\rho^2 \\ -\frac{1}{16}\rho^2 & -\frac{7}{32}\rho^2 & -\frac{29}{64}\rho^2 & -\frac{93}{128}\rho^2 & \frac{251}{64}\rho^2 + \rho & -\frac{386}{512}\rho^2 \\ -\frac{1}{32}\rho^2 & -\frac{8}{64}\rho^2 & -\frac{37}{128}\rho^2 & -\frac{130}{256}\rho^2 & -\frac{386}{512}\rho^2 & \frac{565}{128}\rho^2 + \rho \end{pmatrix}, \quad (68)$$

where we further recall that due to the embedding property the covariance matrices of homogenuose ASIPs of size $n = 1, \ldots, 5$ are all contained in $\mathbf{Cov}[\mathbf{X}(6)]$ as submatrices.

Elements on the main diagonal of the covariance matrix in Eq. (68) are the variances in the site occupancies. These have previously been computed in Ref. [30] and are given by Eq. (16). The nondiagonal elements of the covariance matrix are a measure of the strength of the correlations between pairs of sites in the system. A few simple observations can be made with respect to the latter. First, note that the covariance of the first site with site $j > 1$ is given by

$$(\mathbf{Cov})_{1,j} = -\frac{2}{2^j}\rho^2. \quad (69)$$

Next, note that the covariance of the second site with site $j > 2$ is given by

$$(\mathbf{Cov})_{2,j} = -\frac{j+2}{2^j}\rho^2. \quad (70)$$

The covariance of the third site with site $j > 3$ is given by

$$(\mathbf{Cov})_{3,j} = -\frac{\frac{1}{4}j^2 + \frac{5}{4}j + 2}{2^j}\rho^2. \quad (71)$$

Continuing in this manner, we find that the covariance of site i with site $j > i$ is given by

$$(\mathbf{Cov})_{i,j} = \frac{P_i(j)}{2^j}\rho^2, \quad (72)$$

where

$$
\begin{aligned}
P_1(j) &= -2, \\
P_2(j) &= -j - 2, \\
P_3(j) &= -\tfrac{1}{4}j^2 - \tfrac{5}{4}j - 2, \\
P_4(j) &= -\tfrac{1}{24}j^3 - \tfrac{3}{8}j^2 - \tfrac{4}{3}j - 2, \\
P_5(j) &= -\tfrac{1}{192}j^4 - \tfrac{7}{96}j^3 - \tfrac{83}{192}j^2 - \tfrac{131}{96}j - 2, \\
P_6(j) &= -\tfrac{1}{1920}j^5 - \tfrac{1}{96}j^4 - \tfrac{35}{384}j^3 - \tfrac{11}{24}j^2 - \tfrac{661}{480}j - 2, \\
&\ \ \vdots
\end{aligned}
\tag{73}
$$

The polynomials given in Eq. (73) are the first in an infinite sequence of polynomials. Observe the difference between every pair of consecutive polynomials:

$$
\begin{aligned}
\Delta_1(j) &= P_2(j) - P_1(j) = -j, \\
\Delta_2(j) &= P_3(j) - P_2(j) = -\tfrac{1}{4}j(j+1), \\
\Delta_3(j) &= P_4(j) - P_3(j) = -\tfrac{1}{24}j(j+1)(j+2), \\
\Delta_4(j) &= P_5(j) - P_4(j) = -\tfrac{1}{192}j(j+1)(j+2)(j+3),
\end{aligned}
$$

$$
\begin{aligned}
\Delta_5(j) &= P_6(j) - P_5(j) \\
&= -\tfrac{1}{1920}j(j+1)(j+2)(j+3)(j+4), \\
&\ \ \vdots
\end{aligned}
\tag{74}
$$

We thus find that the polynomial sequence in Eq. (73) is a difference sequence whose differences are of the form $(k > 1)$

$$
\Delta_k(j) = -\frac{j^{(k)}}{2^{k-1}k!},
\tag{75}
$$

where $j^{(k)} = j(j+1)\ldots(j+k-1)$ is the Pochhammer polynomial [52] and $2^{k-1}k!$ is the OEIS sequence A002866. Setting $i < j$ and summing the differences, we obtain a formula for the $P_i(j)$ polynomials:

$$
\begin{aligned}
P_i(j) &= -2 - \sum_{k=1}^{i-1} \frac{j^{(k)}}{2^{k-1}k!} \\
&= 2^{1-i}\binom{i+j-1}{i}{}_2F_1\left(1, i+j; 1+i; \tfrac{1}{2}\right) - 2^{j+1}.
\end{aligned}
\tag{76}
$$

Combining Eqs. (16) and (76) and utilizing the symmetry of the covariance matrix we obtain

$$
(\mathbf{Cov}[\mathbf{X}(n)])_{i,j} =
\begin{cases}
\left(\frac{1}{2^{i+j-1}}\binom{j+i-1}{i}{}_2F_1\left(1, i+j, 1+i; \tfrac{1}{2}\right) - 2\right)\rho^2, & j > i, \\[2mm]
\left(\frac{1}{2^{i+j-1}}\binom{j+i-1}{j}{}_2F_1\left(1, i+j, 1+j; \tfrac{1}{2}\right) - 2\right)\rho^2, & i > j, \\[2mm]
\rho + \left(\frac{4\Gamma(i+1/2)}{\sqrt{\pi}\Gamma(i)} - 1\right)\rho^2, & i = j.
\end{cases}
\tag{77}
$$

The result in Eq. (37) follows immediately.

V. CONCLUSIONS

In this paper, we studied occupancy correlations in the ASIP. We obtained evolution equations for these correlations and introduced an iterative scheme for their computation in the steady-state. Using this scheme, we solved for the steady-state correlations of general ASIPs and obtained a closed-form expression for the correlations of homogeneous ASIPs. In small ASIPs, Monte Carlo simulations provide reliable estimates for occupancy correlations which allowed us to validate our analytical results. As the latter also extend to ASIP systems of arbitrary size, the results we have obtained provide a comprehensive description of spatial correlations in the ASIP which would be virtually impossible to get using brute-force Monte Carlo simulations.

In Figs. 2 and 3, we utilized the results in Eqs. (36) and (37) to explore how occupancy correlations between site i and site j decay with the distance $\Delta = j - i$ between them ($i < j$). For large Δ, this decay was seen to be roughly exponential, but Eqs. (72) and (73) assert that the decay is further modulated by a polynomial of degree $i - 1$, i.e., 1 less than the position of the upstream site i from which the distance between the two sites is measured.

Fixing a distance Δ, one could also ask about the correlation between site i and site $j = i + \Delta$, as this pair is pushed downstream together, i.e., as $i, j \to \infty$. Utilizing Eqs. (36) and (37), we find that for $i, j \gg 1$, $(\mathbf{Cov})_{i,j} \simeq -\lambda^2/\mu_i\mu_j$, which for homogeneous ASIPs boils down to $(\mathbf{Cov})_{i,j} \simeq -\rho^2$. This result asserts that in this limit $\langle X_i X_j \rangle \simeq 0$, which in turn means that two ASIP sites that are located far away downstream are strongly correlated, as they are rarely occupied simultaneously (Fig. 4).
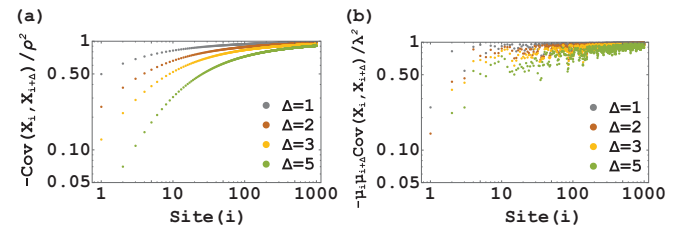

FIG. 4. In the ASIP, the covariance between the occupancy of site i and that of site $i + \Delta$ tends to minus the product of their mean occupancies as $i \to \infty$. We thus have $-\mathbf{Cov}(X_i, X_{i+\Delta}) \simeq \lambda^2/\mu_i\mu_{i+\Delta} = \langle X_i \rangle\langle X_{i+\Delta} \rangle \neq \langle X_i X_{i+\Delta} \rangle \simeq 0$, which suggests strong occupancy correlations in both (a) homogeneous and (b) inhomogeneous ASIP systems. Plots are made using Eqs. (36) and (37).

To better understand the steady-state structure of the ASIP one should go beyond the covariance considered herein. While the full steady-state distribution of the ASIP still poses a formidable challenge, calculating the joint steady-state distribution of site pairs could serve as an interim goal. Specifically, one would like to know $\Pr(X_i = k_i, X_j = k_j)$, i.e., the probability of simultaneously finding k_i particles at site i and k_j particles at site j ($k_i, k_j = 0, 1, 2, 3, \dots$). Generalizing the results obtained herein to ASIP systems with arbitrary, i.e., not necessarily exponential, gate opening times is also of interest [31]. Doing so will require methods that go beyond those used above.

Finally, we turn our attention to the fact that the analysis conducted herein was focused on situations where all gate opening rates in the ASIP are known and fixed. In particular, by homogeneous ASIP systems we mean ASIP systems in which all gate opening rates are strictly identical. However, similarly to the ASEP and related exclusion models [53–59], one may also consider disordered ASIP systems where, e.g.,

gate opening rates are not identical per se but, rather, identically distributed around a given mean. Studying the statistical properties of such ASIP systems is of interest since small, and seemingly random, differences in transition rates may arise in applications for various reasons. The resulting random covariance matrices will then form a statistical ensemble that can, in principle, be tackled with tools coming from random matrix theory. In turn, this approach may lead to the discovery of interesting phenomena and statistical universality in the ASIP, as has also occurred elsewhere [60–68].

ACKNOWLEDGMENTS

[1] S. Reuveni, I. Eliazar, and U. Yechiali, Asymmetric inclusion process, Phys. Rev. E **84**, 041101 (2011).

[2] S. Reuveni, I. Eliazar, and U. Yechiali, The Asymmetric Inclusion Pprocess: A Showcase of Complexity, Phys. Rev. Lett. **109**, 020603 (2012).

[3] R. R. P. Jackson, Queueing systems with phase-type service, Operat. Res. Q. **5**, 109 (1954).

[4] R. R. P. Jackson, Random queueing processes with phase-type service, J. Roy. Stat. Soc. Ser. B (Methodol.) **18**, 129 (1956).

[5] M. Harchol-Balter, *Performance Modeling and Design of Computer Systems: Queueing Theory in Action* (Cambridge University Press, Cambridge, UK, 2013).

[6] D. G. Kendall, Stochastic processes occurring in the theory of queues and their analysis by the method of the imbedded Markov chain, Ann. Math. Stat. **24**, 338 (1953).

[7] B. Derrida, E. Domany, and D. Mukamel, An exact solution of the one dimensional asymmetric exclusion model with open boundaries, J. Stat. Phys. **69**, 667 (1992).

[8] O. Golinelli and K. Mallick, The asymmetric simple exclusion process: An integrable model for non-equilibrium statistical mechanics, J. Phys. A: Math. Gen. **39**, 12679 (2006).

[9] B. Derrida, Non-equilibrium steady-states: Fluctuations and large deviations of the density and of the current, J. Stat. Mech. P07023 (2007).

[10] R. A. Blythe and M. R. Evans, Nonequilibrium steady-states of matrix-product form: a solver's guide, J. Phys. A: Math. Theor. **40**, R333 (2007).

[11] C. T. MacDonald, J. H. Gibbs, and A. C. Pipkin, Kinetics of biopolymerization on nucleic acid templates, Biopolymers **6**, 1 (1968).

[12] F. Spitzer, Interaction of Markov processes, Adv. Math. **5**, 246 (1970).

[13] K. Heckmann, Single File, in *Biomembranes: Passive Permeability of Cell Membranes*, edited by F. Kreuzer and J. F. G. Slegers, Biomembranes (Springer, Boston, MA, 1972), Vol. 3, pp. 127–153.

[14] D. G. Levitt, Dynamics of a single-file pore: Non-Fickian behavior, Phys. Rev. A **8**, 3050 (1973).

[15] P. M. Richards, Theory of one-dimensional hopping conductivity and diffusion, Phys. Rev. B **16**, 1393 (1977).

[16] B. Widom, J. L. Viovy, and A. D. Defontaines, Repton model of gel electrophoresis and diffusion, J. Phys. I (France) **1**, 1759 (1991).

[17] M. Schreckenberg and D. E. Wolf (eds.), *Traffic and Granular Flow* (Springer, Berlin, 1998).

[18] S. Reuveni, I. Meilijson, M. Kupiec, E. Ruppin, and T. Tuller, Genome-scale analysis of translation elongation with a ribosome flow mode, PLoS Comput. Biol. **7**, e1002127 (2011).

[19] L. B. Shaw, R. K. Zia, and K. H. Lee, Totally asymmetric exclusion process with extended objects: A model for protein synthesis, Phys. Rev. E **68**, 021910 (2003).

[20] T. Halpin-Healy and Y. C. Zhang, Kinetic roughening phenomena, stochastic growth, directed polymers and all that, Phys. Rep. **254**, 215 (1995).

[21] J. Krug, Origins of scale invariance in growth processes, Adv. Phys. **46**, 139 (1997).

[22] R. Bundschuh, Asymmetric exclusion process and extremal statistics of random sequences, Phys. Rev. E **65**, 031911 (2002).

[23] S. Klumpp and R. Lipowsky, Traffic of molecular motors through tube-like compartments, J. Stat. Phys. **113**, 233 (2003).

[24] S. F. Burlatsky, G. S. Oshanin, A. V. Mogutov, and M. Moreau, Directed walk in a one-dimensional lattice gas, Phys. Lett. A **166**, 230 (1992).

[25] S. F. Burlatsky, G. Oshanin, M. Moreau, and W. P. Reinhardt, Motion of a driven tracer particle in a one-dimensional symmetric lattice gas, Phys. Rev. E **54**, 3165 (1996).

[26] O. Bénichou, A. M. Cazabat, J. De Coninck, M. Moreau, and G. Oshanin, Stokes Formula and Density Perturbances for Driven Tracer Diffusion in an Adsorbed Monolayer, Phys. Rev. Lett. **84**, 511 (2000).

[27] C. M. Monasterio and G. Oshanin, Bias and bath mediated pairing of particles driven through a quiescent medium, Soft Matter **7**, 993 (2011).

[28] B. Derrida, M. R. Evans, V. Hakim, and V. Pasquier, Exact solution of a 1d asymmetric exclusion model using a matrix formulation, J. Phys. A **26**, 1493 (1993).

[29] S. Reuveni, I. Eliazar, and U. Yechiali, Limit laws for the asymmetric inclusion process, Phys. Rev. E **86**, 061133 (2012).

[30] S. Reuveni, O. Hirschberg, I. Eliazar, and U. Yechiali, Occupation probabilities and fluctuations in the asymmetric simple inclusion process, Phys. Rev. E **89**, 042109 (2014).

[31] O. Boxma, O. Kella, and U. Yechiali, An ASIP model with general gate opening intervals, Queue. Syst. **84**, 1 (2016).

[32] S. Grosskinsky, F. Redig, and K. Vafayi, Condensation in the inclusion process and related models, J. Stat. Phys. **142**, 952 (2011).

[33] J. Cao, P. Chleboun, and S. Grosskinsky, Dynamics of condensation in the totally asymmetric inclusion process, J. Stat. Phys. **155**, 523 (2014).

[34] M. F. Neuts, The busy period of a queue with batch service, Operat. Res. **13**, 815 (1965).

[35] H. Kaspi, O. Kella, and D. Perry, Dam processes with state dependent batch sizes and intermittent production processes with state dependent rates, Queue. Syst.: Theory Appl. **24**, 37 (1997).

[36] O. Boxma, D. Perry, W. Stadje, and S. Zacks, A Markovian growth-collapse model, Adv. Appl. Prob. **38**, 221 (2006).

[37] O. Kella, On growth collapse processes with stationary structure and their shot-noise counterparts, J. Appl. Prob. **46**, 363 (2009).

[38] B. J. Martin, Batch queues, reversibility and first-passage percolation, Queue. Syst.: Theory Appl. **62**, 411 (2009).

[39] P. Bak, *How Nature Works: The Science of Self-Organized Criticality* (Springer-Verlag, New York, 1996).

[40] M. G. Rozman, M. Urbakh, J. Klafter, and F. J. Elmer, Atomic scale friction and different phases of motion of embedded molecular systems, J. Phys. Chem. B **102**, 7924 (1998).

[41] J. M. Carlson, J. S. Langer, and B. E. Shaw, Dynamics of earthquake faults, Rev. Mod. Phys. **66**, 657 (1994).

[42] I. Eliazar and J. Klafter, A growth-collapse model: Lévy inflow, geometric crashes, and generalized Ornstein-Uhlenbeck dynamics, Physica A **334**, 1 (2004).

[43] I. Eliazar and J. Klafter, Stochastic Ornstein-Uhlenbeck capacitors, J. Stat. Phys. **118**, 177 (2005).

[44] I. Eliazar and J. Klafter, Growth-collapse and decay-surge evolutions, and geometric Langevin equations, Physica A **367**, 106 (2006).

[45] M. Smoluchowski, Versuch einer mathematischen Theorie der Koagulationskinetik kolloider Lösungen, Z. Phys. Chem. **92**, 129 (1917).

[46] I. M. Sokolov, S. B. Yuste, J. J. Ruiz-Lorenzo, and K. Lindenberg, Mean field model of coagulation and annihilation reactions in a medium of quenched traps: Subdiffusion, Phys. Rev. E **79**, 051113 (2009).

[47] S. B. Yuste, J. J. Ruiz-Lorenzo, and K. Lindenberg, Coagulation reactions in low dimensions: Revisiting subdiffusive A + A reactions in one dimension, Phys. Rev. E **80**, 051114 (2009).

[48] P. L. Krapivsky, S. Redner, and E. Ben-Naim, *A Kinetic View of Statistical Physics* (Cambridge University Press, Cambridge, UK, 2010).

[49] D. Ben-Avraham. The coalescence process, $A + A \rightarrow A$, and the method of interparticle distribution functions, in *Nonequilibrium Statistical Mechanics in One Dimension*, edited by V. Privman (Cambridge University Press, Cambridge, UK, 2005), pp. 29–50.

[50] M. R. Evans and T. Hanney, Nonequilibrium statistical mechanics of the zero-range process and related models, J. Phys. A **38**, R195 (2005).

[51] S. Reuveni, Catalan's trapezoids, Probab. Eng. Info. Sci. **28**, 353 (2014).

[52] M. Abramowitz, and I. A. Stegun, *Handbook of Mathematical Functions: With Formulas, Graphs, and Mathematical Tables*, Vol. 55 (Courier Corp., Chelmsford, MA, 1965).

[53] J. Krug, Phase separation in disordered exclusion models, Braz. J. Phys. **30**, 97 (2000).

[54] R. J. Harris, and R. B. Stinchcombe, Disordered asymmetric simple exclusion process: Mean-field treatment, Phys. Rev. E **70**, 016108 (2004).

[55] M. R. Evans, T. Hanney, and Y. Kafri, Disorder and nonconservation in a driven diffusive system, Phys. Rev. E **70**, 066124 (2004).

[56] R. Juhász, L. Santen, and F. Iglói, Partially Asymmetric Exclusion Models with Quenched Disorder, Phys. Rev. Lett. **94**, 010601 (2005).

[57] M. Barma, Driven diffusive systems with disorder, Physica A: Stat. Mech. Appl. **372**, 22 (2006).

[58] M. E. Foulaadvand, S. Chaaboki, and M. Saalehi, Characteristics of the asymmetric simple exclusion process in the presence of quenched spatial disorder, Phys. Rev. E **75**, 011127 (2007).

[59] M. E. Foulaadvand, A. B. Kolomeisky, and H. Teymouri, Asymmetric exclusion processes with disorder: Effect of correlations, Phys. Rev. E **78**, 061116 (2008).

[60] T. Tao, *Topics in Random Matrix Theory*, Vol. 132 (American Mathematical Society, Providence, RI, 2012).

[61] L. Laloux, P. Cizeau, M. Potters, and J. P. Bouchaud, Random matrix theory and financial correlations, Int. J. Theor. Appl. Finance **3**, 391 (2000).

[62] V. Plerou, P. Gopikrishnan, B. Rosenow, L. A. N. Amaral, T. Guhr, and H. E. Stanley, Random matrix approach to cross correlations in financial data, Phys. Rev. E **65**, 066126 (2002).

[63] D. S. Dean and S. N. Majumdar, Large Deviations of Extreme Eigenvalues of Random Matrices, Phys. Rev. Lett. **97**, 160201 (2006).

[64] G. Biroli, J. P. Bouchaud, and M. Potters, Extreme value problems in random matrix theory and other disordered systems, J. Stat. Mech. (2007) P07019.

[65] S. N. Majumdar and M. Vergassola, Large Deviations of the Maximum Eigenvalue for Wishart And Gaussian Random Matrices, Phys. Rev. Lett. **102**, 060601 (2009).

[66] J. Bun, J. P. Bouchaud, and M. Potters, Cleaning large correlation matrices: Tools from random matrix theory, Phys. Rep. **666**, 1 (2017).

[67] I. Eliazar, R. Metzler, and S. Reuveni, Gumbel central limit theorem for max-min and min-max, Phys. Rev. E **100**, 020104(R) (2019).

[68] I. Eliazar, R. Metzler, and S. Reuveni, Poisson-process limit laws yield Gumbel max-min and min-max, Phys. Rev. E **100**, 022129 (2019).